

## Self-assembly of versatile tubular-like $\text{In}_2\text{O}_3$ nanostructures

To cite this article: Miao Zhong *et al* 2007 *Nanotechnology* **18** 465605

View the [article online](#) for updates and enhancements.

### You may also like

- [Field-effect transistors engineered via solution-based layer-by-layer nanoarchitectonics](#)

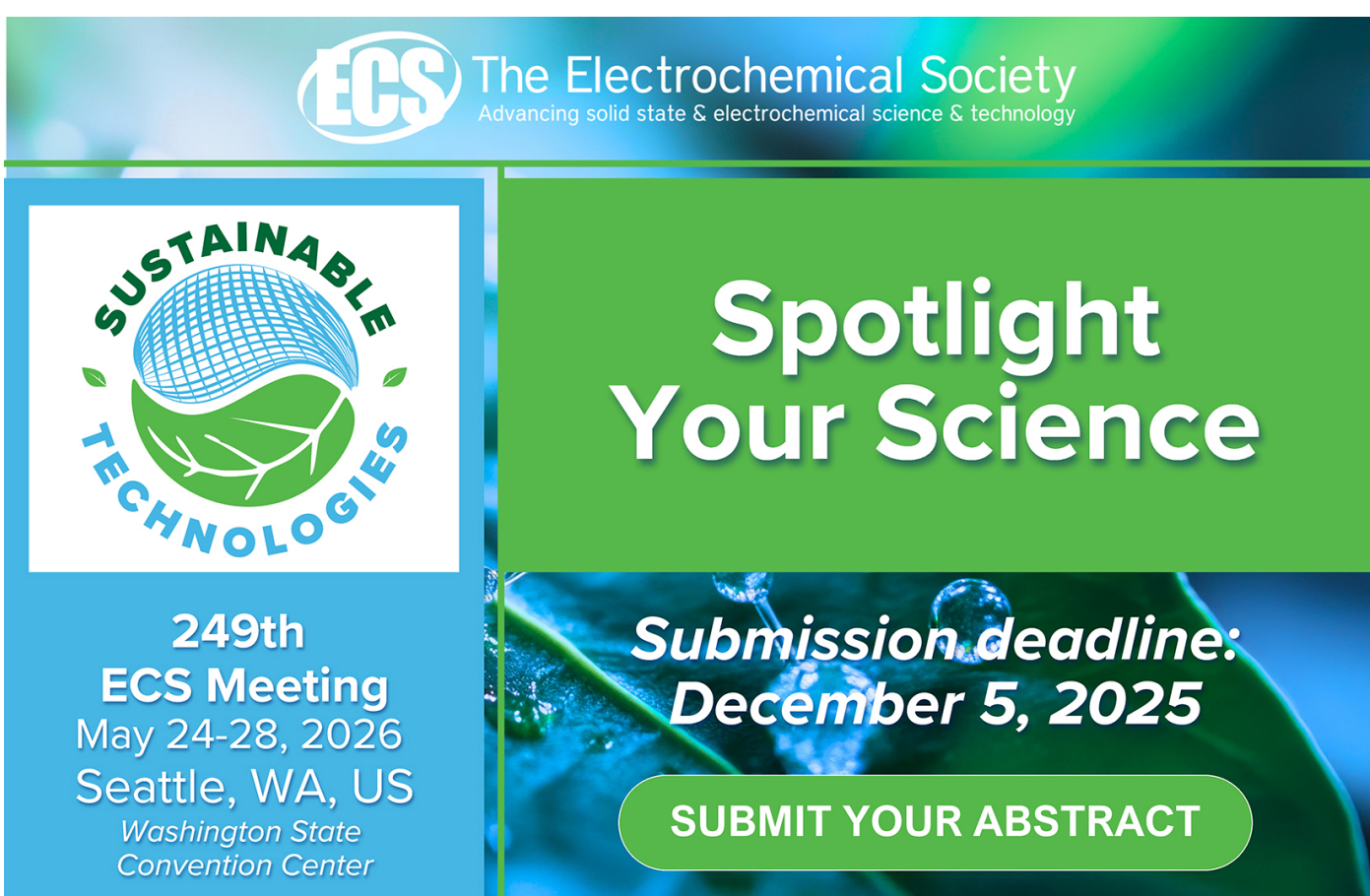
Omar Azzaroni, Esteban Piccinini, Gonzalo Fenoy *et al.*

- [Deep-ultraviolet integrated photonic and optoelectronic devices: A prospect of the hybridization of group III-nitrides, III–oxides, and two-dimensional materials](#)

Nasir Alfaraj, Jung-Wook Min, Chun Hong Kang *et al.*

- [Damage sensing in multi-functional nanocomposite polymer bonded energetics with embedded multi-walled carbon nanotube sensing networks](#)

Nishant Shirodkar, Viswajit Talluru and Gary D Seidel



The Electrochemical Society  
Advancing solid state & electrochemical science & technology

**ECS**

**SUSTAINABLE TECHNOLOGIES**

**249th ECS Meeting**  
May 24-28, 2026  
Seattle, WA, US  
Washington State Convention Center

**Spotlight Your Science**

**Submission deadline:**  
**December 5, 2025**

**SUBMIT YOUR ABSTRACT**

# Self-assembly of versatile tubular-like $\text{In}_2\text{O}_3$ nanostructures

Miao Zhong<sup>1</sup>, Maojun Zheng<sup>1,3</sup>, Li Ma<sup>2</sup> and Yanbo Li<sup>1</sup>

<sup>1</sup> Laboratory of Condensed Matter Spectroscopy and Opto-Electronic Physics, Department of Physics, Shanghai Jiao Tong University, Shanghai 200240, People's Republic of China

<sup>2</sup> School of Chemistry and Chemical Technology, Shanghai Jiao Tong University, Shanghai 200240, People's Republic of China

E-mail: mjzheng@sjtu.edu.cn

Received 8 August 2007, in final form 16 September 2007

Published 12 October 2007

Online at [stacks.iop.org/Nano/18/465605](http://stacks.iop.org/Nano/18/465605)

## Abstract

Versatile indium oxide tubular nanostructures (well-aligned nanotube arrays, flower-like tubular structures, and square nanotubes) were fabricated by a facile and reliable chemical vapor deposition (CVD) technique, taking advantage of the self-assembly property and substrate-induced epitaxial growth mechanism. The technique has a few advantages, such as low growth temperature, nonexistence of catalyst, template-free synthesis, direct bonding to the semiconductor substrates, etc. This strategy might extend the approach of synthesizing desirable nanostructures of other important low-melting metal oxides for potential applications.

## 1. Introduction

Since the discovery of carbon nanotubes (NTs) in 1991 [1], tubular structures have become of great interest because of their unique properties and numerous potential applications in optoelectronic devices, biological devices, gas sensors, advanced catalysis and energy storage [2–8]. Up to now, various physical and chemical approaches have been developed to fabricate quasi-tubular formations, such as laser ablation [9], the solution-phase route [10], the gelation process [11], chemical vapor deposition [12–14], etc. However, an intermedia catalyst or a high process temperature is necessary in some of these methods. In order to fabricate highly aligned nanotubes, considerable attempts are currently focused on template-originated methods [15–18], which mostly utilize a tubular template of an organogelator or surfactant to encapsulate oxides or use a nanoporous alumina/carbon template as the substrate to fabricate nanotubes of oxides. However, there still exists the problem of removing the templates without destroying the as-prepared structures. Also, impure components always remain with the oxides.

Indium oxide, a useful wide-band-gap transparent semiconductor, has aroused much attention due to its interesting properties in many important industry fields [19–21]. However, most of the research is concentrated on constructing

artificial nanostructures of nanowires or nanoneedles; there has been less reported on nanotube alignments. In this paper, we demonstrate a simple but effective CVD technique to construct versatile indium oxide tubular nanostructures: well-aligned nanotube (NT) arrays, flower-like tubular structures, and square NTs. This method has a few advantages, such as substrate-induced epitaxial growth, a structured pattern depending strongly on tunable conditions and self-assembly growth processes, low growth temperature, nonexistence of catalyst, direct bonding to the semiconductor substrates, etc. We consider that it might provide a new route for low-melting temperature metals to directly synthesize desirable structures with controlled composition, crystallinity, and morphology.

## 2. Experimental details

The synthesis approach for the diverse tubular nanostructures of  $\text{In}_2\text{O}_3$  is briefly composed of two steps: preparation of a high-quality nanoporous substrate of InP and epitaxial growth of  $\text{In}_2\text{O}_3$  nanostructures via the CVD process. As reported in our previous work [22], large-scale uniform InP nanopore arrays were fabricated by means of electrochemical anodization in HCl solution. Then, the prepared porous InP (with indium source), loaded in a ceramic boat, was put into the center of a horizontal quartz tube of a tubular furnace. First, the quartz tube was evacuated for 10 min by a mechanical pump. Then the samples were annealed

<sup>3</sup> Author to whom any correspondence should be addressed.

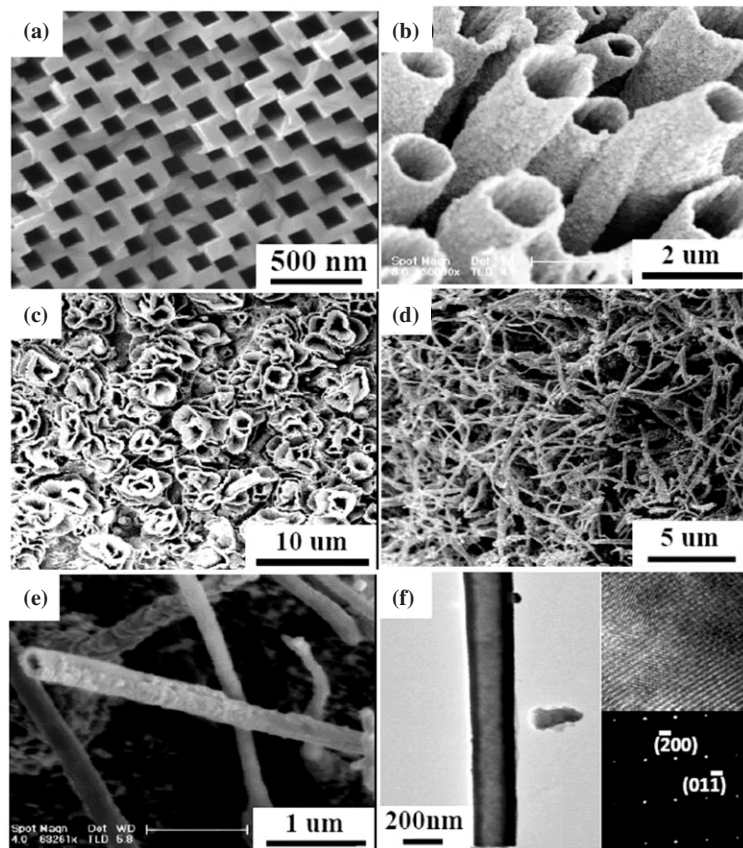


**Figure 1.** (a) Plan-view SEM image of square-shaped nanopore arrays of InP. (b)–(e) SEM images of diverse In<sub>2</sub>O<sub>3</sub> tubular structures. (f) TEM image of nanotubes from the same sample of image (d); the images on the right are its corresponding SAED pattern and HRTEM image.

**Table 1.** Experimental details and obtained morphologies.

Source	Process	Morphology
Porous InP	Condition 1, 500 °C	Vertical In <sub>2</sub> O <sub>3</sub> nanotube arrays
Porous InP and In	Condition 1, 600 °C	Flower-like tubular structures
Porous InP and In	Condition 2	Square NTs

under different conditions (condition 1: pre-heat the sample at 450 °C for 1 h in low vacuum conditions, then raise the temperature to 500 °C/600 °C, and hold for 2 h with Ar and O<sub>2</sub> gas flowing at a rate of 240 and 80 sccm; condition 2: directly heat the sample at 600 °C with Ar and O<sub>2</sub> gas kept flowing in at the same rate). After the annealing treatments, the furnace was naturally cooled down to room temperature, and three different kinds of large-scale In<sub>2</sub>O<sub>3</sub> nanostructures were obtained. (The particular details and corresponding morphologies are summarized in table 1.)

### 3. Results and discussion

Figure 1(a) shows a typical scanning electron microscopy (SEM) image of uniform and square InP nanopore arrays. The average inner diameter (diagonal length) of pores and the average wall thickness of the pores were estimated to be 120 nm and 75 nm, respectively. Utilizing such a geometric

surface as substrate, different kinds of tubular structure of In<sub>2</sub>O<sub>3</sub> are synthesized via the consequent CVD process. Figure 1(b) shows an SEM image of vertical In<sub>2</sub>O<sub>3</sub> NT arrays. It shows that the aligned tubes grow straightly on the substrate, with diameters around 800 nm–1.2 μm and length around 2–6 μm. Figure 1(c) shows an SEM image of the flower-like tubular structure of In<sub>2</sub>O<sub>3</sub>. The individual multilayered flower-like structure consists of densely packed nanotubes. Each layer of the petal-like tube is smooth and radially oriented, with an outer diameter around 3–5 μm. Figures 1(d) and (e) demonstrate ultralong square In<sub>2</sub>O<sub>3</sub> NTs at different magnifications. Figure 1(d) is a low-magnification view of the product, revealing that the NTs are widespread over the whole substrate with random directions. Figure 1(e) shows a close-up view of one single NT at a higher magnification, from which the obviously square and opened-up nozzle can be observed at one end of the NT, corresponding to the morphology and dimension of the InP nanopores. This clone structure indicates that square NTs are directly developed from the InP substrate.

Such structure was further investigated by transmission electron microscopy (TEM) and high-resolution transmission electron microscopy (HRTEM) images. Figure 1(f) shows the TEM (JEOL JEM-2100F) image of a single NT with a high degree of contrast between the bright central part and the dark edges, which represent the hollow character of the tube. The outer diameters of the nanotubes are around 200–300 nm, retaining the size and similar square shape of the pores

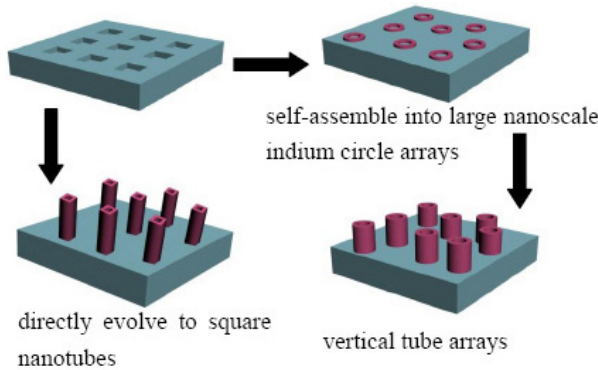


**Figure 2.** Schematic depiction of the formation of tubular structures.  
(This figure is in colour only in the electronic version)

of the InP substrates. The tube body is uniformly straight and smooth with no macroscopic defects. Its selected area electron diffraction (SAED) pattern (images on the right-hand side of figure 1(f)) indicates that the fine structure is single-crystalline and that it grew along the [100] direction. High-resolution TEM (HRTEM) was employed to confirm the highly crystallized character. The interplanar spacing of  $\sim 0.413$  nm agrees well with the spacing of the (211) planes of  $\text{In}_2\text{O}_3$  crystal.

We postulate that the nucleation and growth of vertical NT arrays occurs in three basic steps: (1) dissolution of nanoporous InP, (2) self-assembly organization of large nanoscale circles of molten indium, (3) dynamic formation of  $\text{In}_2\text{O}_3$  nuclei circles and homoepitaxial growth of  $\text{In}_2\text{O}_3$  tubular structures. A simple mode for the dynamic growth illustration is proposed, as shown in figure 2. When the furnace temperature was increased to  $450^\circ\text{C}$  and maintained for 1 h in low vacuum conditions in the pre-heating step, a rapid dissolution process of nanoporous InP took place. Phosphor vapor was drawn out by the vacuum pump, while indium remained on the surface of substrate in liquid state. Via this step, indium droplets on the surface spontaneously coalesced together to form closed circles with large nanoscale diameter. There is one particular question: why were the large nanoscale circles circular-shaped rather than other shapes? It is reasonable to assume that this might be related to the combinational effects of substrate-inducement (porous morphology, stress, etc) and self-assembly characters. With the reactant gas  $\text{O}_2$  flowing into the chamber, the molten indium circles on the surface first reacted with  $\text{O}_2$  to synthesize the  $\text{In}_2\text{O}_3$  ring-shaped nuclei and then they gradually developed into tubular structures. With time, the length of tubes increased. Meanwhile, the length of tube increased which prevented other nucleation of  $\text{In}_2\text{O}_3$  inside the tubes by reducing the probability of  $\text{O}_2$  and indium meeting. Thus, the continuous decomposition of porous parts beneath or inside the  $\text{In}_2\text{O}_3$  circles, acted as an indium source, and kept the growth of the  $\text{In}_2\text{O}_3$  nanotube.

In order to prove the hypothesis of decomposition of InP and growth of  $\text{In}_2\text{O}_3$ , an x-ray diffraction system (XRD) was employed to investigate the surface parts of the porous InP substrate at various stages during the growth process. A comparison of XRD results is presented in figure 3. Figure 3(a)

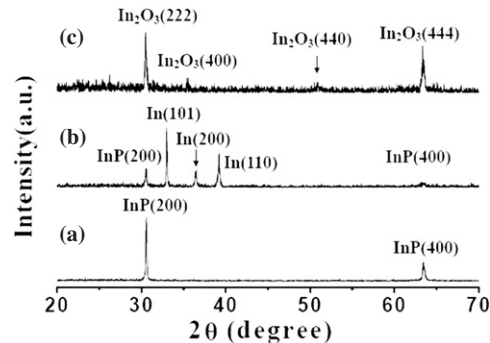


**Figure 3.** X-ray diffraction (XRD) patterns of porous InP treated at different conditions. (a) XRD result from porous InP substrate. (b) XRD result from porous InP pre-heated in a low-vacuum chamber at  $450^\circ\text{C}$  for 1 h. (c) XRD result from products of  $\text{In}_2\text{O}_3$  nanotube arrays.

is the original diffraction spectrum of porous InP; figure 3(b) shows the result after pre-heating InP at  $450^\circ\text{C}$  for 1 h, which indicates that porous InP substrate is decomposed. Phosphor was evacuated while indium stayed on the surface, which supports the supposition of dissolution before. Figure 3(c) shows a typical diffraction pattern of the final  $\text{In}_2\text{O}_3$  product. No other element such as indium or phosphor was detected.

It is worth noting that porous structures of InP substrates herein play key roles. First, they lower the decomposition temperature for easier control of the growth of  $\text{In}_2\text{O}_3$  nanotubes. Second, they confine the fluidity of molten indium so as to facilitate the self-assembly formation of molten indium circles via the pre-heating step. In contrast, during the same annealing disposal to bulk InP with a smooth surface, molten indium joined together into irregular morphologies and none of the nanostructures was obtained. Third, they make the  $\text{In}_2\text{O}_3$  NT grow homoepitaxially along the porous direction, ensuring growth perpendicular to the substrate plane.

By altering the growth condition, a flower-like structure of  $\text{In}_2\text{O}_3$  was obtained. In contrast to the growth process of vertical nanotube arrays of  $\text{In}_2\text{O}_3$ , extra indium was added as external source and the annealing temperature was raised to  $600^\circ\text{C}$  in the fabrication of a flower-like structure, which could result in indium vapor being supersaturated in the chamber. We postulate that large indium vapor supersaturation could cause multi-dimensional nucleation of  $\text{In}_2\text{O}_3$  on the molten indium circles, which gradually evolved into branched nucleation circles [23, 24], which led to the growth direction of the tubular nanostructures multiplex. In addition, the increasing annealing temperature is another influential factor which boosted the reaction speed of indium and oxygen, causing the nucleation and growth orientation to be uncertain and difficult to control. After the whole growth process, multiple nanotubes packed densely, and a flower-like tubular structure was formed.

In the square NT growth process, porous InP substrate was directly annealed at  $600^\circ\text{C}$  for 2 h with Ar and  $\text{O}_2$  gas constantly flowing without the pre-treatment step. The high annealing temperature of  $600^\circ\text{C}$  was used to enhance the decomposition speed of porous InP and reaction speed between indium and oxygen. The molten indium decomposed from InP diffusing into InP, and formed a eutectic on the surface part of the porous wall, facilitating the formation of  $\text{In}_2\text{O}_3$  nuclei.

And extra indium grains were employed to increase the indium vapor density to assure the reaction possibility of indium and O<sub>2</sub> for maintaining the growth. Thus, it is deduced that the decomposition of InP and nucleation of In<sub>2</sub>O<sub>3</sub> herein occurred simultaneously and continuously. Gradually, the square NTs were obtained, as described in figure 2. However, increasing the NT's length and raising the temperature resulted in the growth direction of In<sub>2</sub>O<sub>3</sub> NTs being ungovernable, so that all the NTs are curved with an arbitrary growth orientation. In a word, the controllable experiment factors, such as reaction steps, annealing temperature and extra source, have great effects in the fabrication of various structures.

#### 4. Conclusion

In summary, we have presented a facile and controllable method for the large-scale fabrication of diverse In<sub>2</sub>O<sub>3</sub> tubular nanostructures. This available strategy of utilizing self-assembly and substrate-induced properties allowed for template-free synthesis of a vertically arrayed nanotube pattern. Furthermore, flower-like tubular structures and square nanotubes were also successfully fabricated by intentionally altering the growth conditions. We suggest that this technique might provide a conceptually different route for synthesizing desirable nanostructures of other important low-melting point metal oxides for practical application.

#### Acknowledgments

This work was supported by the Natural Science Foundation of China (Grant no. 50572064) and the National Minister of Education Program for Changjiang Scholars and Innovative Research Team in University (PCSIRT).

#### References

- [1] Iijima S 1991 *Nature* **354** 56–8
- [2] Lu J G, Chang P and Fan Z 2006 *Mater. Sci. Eng. Rep.* **52** 49–91
- [3] Reches M and Gazit E 2003 *Science* **300** 625–7
- [4] van Bommel K J C, Friggeri A and Shinkai S 2003 *Angew. Chem. Int. Edn* **42** 980–99
- [5] Chopra N G, Luyken R J, Cherrey K, Crespi V H, Cohen M L, Louie S G and Zettl A 1995 *Science* **269** 966–7
- [6] Suenaga K, Colliex C, Demoncey N, Loiseau A, Pascard H and Willaime F 1997 *Science* **278** 653–5
- [7] Remskar M, Mrzel A, Skraba Z, Jesih A, Ceh M, Demšar J, Stadelmann P, Le'vy F and Mihailovic D 2001 *Science* **292** 479–81
- [8] Hacohen Y R, Grunbaum E, Tenne R, Sloan J and Hutchison J L 1998 *Nature* **395** 336–7
- [9] Bakkers E P A M and Verheijen M A 2002 *J. Am. Chem. Soc.* **125** 3440–1
- [10] Wang Z, Qian X, Yin J and Zhu Z 2004 *Langmuir* **20** 3441–8
- [11] Lee H Y, Nam S R and Hong J 2007 *J. Am. Chem. Soc.* **129** 1040–1
- [12] Sharma S and Sunkare M K 2002 *J. Am. Chem. Soc.* **124** 12288–93
- [13] Zhang B P, Binh N T, Wakatsuki K, Segawa Y, Ymada Y, Usami N, Kawasaki M and Koinuma H 2004 *Appl. Phys. Lett.* **84** 4098
- [14] Huang S, Woodson M, Smalley R and Liu J 2004 *Nano Lett.* **4** 1025–8
- [15] Rao C N R, Satishkumar B C and Govindaraj A 1997 *Chem. Commun.* **16** 1581
- [16] Li Y, Bando Y and Golberg D 2003 *Adv. Mater.* **15** 581–5
- [17] Kobayashi S, Hamasaki N, Suzuki M, Kimura M, Shirai H and Hanabusa K 2002 *J. Am. Chem. Soc.* **124** 6550–1
- [18] Fan X, Meng X, Zhang X, Lee C and Lee S 2007 *Appl. Phys. Lett.* **90** 103114
- [19] Pan Z W, Dai Z R and Wang Z L 2001 *Science* **291** 1947–9
- [20] Peng X S, Meng G W, Zhang J, Wang X F, Wang Y W, Wang C Z and Zhang L D 2002 *J. Mater. Chem.* **12** 1602–5
- [21] Zheng M J, Zhang L D, Li G H, Zhang X Y and Wang X F 2001 *Appl. Phys. Lett.* **79** 839–41
- [22] Zeng A S, Zheng M J, Ma L and Shen W Z 2006 *Nanotechnology* **17** 4163–7
- [23] Ozturk B, Talukdar I and Flanders B N 2007 *Nanotechnology* **18** 365302
- [24] Liang Y X, Li S Q, Nie L, Wang Y G and Wang T H 2006 *Appl. Phys. Lett.* **88** 193119